Domain growth and freezing on a triangular lattice

H. C. Kang* and W. H. Weinberg*
Division of Chemistry and Chemical Engineering, California Institute of Technology, Pasadena, California 91125
(Received 2 December 1988)

We have performed Monte Carlo simulations of domain growth at zero temperature of a lattice gas with nearest-neighbor repulsive interactions on a triangular lattice. Kawasaki dynamics were used with a fractional surface coverage of one-third. We studied both the case in which the second-nearest-neighbor interaction is attractive and the case in which it is zero. The effect of increasing the range of allowed hops from nearest neighbor to third nearest neighbor was investigated. We find that domain growth freezes in the case in which the second-nearest-neighbor interaction is attractive and only nearest-neighbor hops are allowed. Domain freezing is released when longer-range hops are allowed or when the second-nearest-neighbor interaction is zero. Allowing only nearest-neighbor hops, the growth exponent when there is no second-nearest-neighbor interaction is consistent with the Lifshitz-Slyozov theory. We conclude that the range of particle hops is an important parameter to consider when classifying growth kinetics.

I. INTRODUCTION

The kinetics of domain growth in systems that have been quenched below an ordering temperature T_c has been widely studied.[1] There has been considerable interest recently in the kinetics of domain growth at zero temperature, with particular focus on the freezing of domain sizes.[2–6] A combination of Monte Carlo simulations and renormalization-group methods was employed[3] to study the ferromagnetic Ising model, $H=J_{\mathrm{NN}}\sum_{(i\neq j)_{\mathrm{NN}}}s_i s_j$.[7] Using Kawasaki dynamics, it was found that the domain size freezes at zero temperature. A similar method was used[4] to study the eight-state Potts model on a square lattice, with the Hamiltonian

$$H=J_{\mathrm{NN}}\sum_{(i\neq j)_{\mathrm{NN}}}\delta_{s_i s_j}+J_{\mathrm{NNN}}\sum_{(i\neq j)_{\mathrm{NNN}}}\delta_{s_i s_j}$$

(Ref. 8). Two "fixed points" at $T=0$ were found; one is a freezing "fixed point" for $J_{\mathrm{NNN}}/J_{\mathrm{NN}}\neq 1$, and the other is the equilibration "fixed point" for $J_{\mathrm{NNN}}/J_{\mathrm{NN}}=1$. It was concluded that the attractive "fixed point" for quenches to finite temperatures is the equilibration "fixed point." Another Hamiltonian which has been investigated is

$$H=J_{\mathrm{NN}}\sum_{(i\neq j)_{\mathrm{NN}}}s_i s_j+J_{\mathrm{NNN}}\sum_{(i\neq j)_{\mathrm{NNN}}}s_i s_j$$

on a square lattice with J_{NN} and J_{NNN} both positive. Using Glauber dynamics, it was found that for $\alpha=J_{\mathrm{NNN}}/J_{\mathrm{NN}}<1$, domain freezing occurs; whereas for $\alpha\geq 1$, the growth exponent x is approximately $\frac{1}{2}$.[5] At finite temperatures, the domain-growth freezing is released. Using the same Hamiltonian with $\alpha=1$, but using spin-exchange dynamics, it was found that the domain size freezes when only nearest-neighbor spin exchanges are allowed.[6] If second-nearest-neighbor spin exchanges are also allowed, the freezing is released.

Some general conclusions concerning domain growth have been drawn from these studies. It was suggested that the freezing of domain growth at zero temperature implies that the growth law at finite temperatures below the critical temperatures is $l\sim\ln t$.[3] However, this has not been observed in simulations either for (2×1) ordered domains on a square lattice[9] or for $(\sqrt{3}\times\sqrt{3})$ (Ref. 10) ordered domains on a triangular lattice.[11] The simulations of the growth of (2×1) domains on a square lattice show $l\sim t^x$, with a temperature-dependent x for temperatures close to zero. This temperature dependence has been interpreted in two different ways. Sadiq and Binder[9,12] concluded that there is a "crossover" from $x=0$ at zero temperature to a finite value, probably $x=\frac{1}{3}$, for all nonzero temperatures. The temperature dependence that is observed in simulations is thought to arise because the simulations have not yet reached the asymptotic regime in which the true growth exponent would be observed, and the time it would take to reach this asymptotic regime becomes longer as the temperature becomes lower. Using a precursor-mediated mechanism for domain growth, it has been found that the growth exponents obtained from Monte-Carlo simulations are strongly dependent on the mobility of the precursors.[13] It has also been found that the freezing of the growth of (2×1) domains, using Kawasaki dynamics, on a square lattice at zero temperature is released if second-nearest-neighbor hops are allowed.[6] The growth exponent that was obtained is close to $\frac{1}{2}$, and it was suggested that the actual growth exponent for (2×1) domains on a square lattice is $\frac{1}{2}$. It was argued that the conflicting observations of Sadiq and Binder[9] resulted because their simulations were not sufficiently long to probe the asymptotic regime. Since the density is conserved in the simulations allowing second-nearest-neighbor hops with Kawasaki dynamics, the value of approximately $\frac{1}{2}$ for the growth exponent of (2×1) domains on a square lattice led to the conclusion[6] that density conservation is irrelevant for degeneracies greater than two.

Recent work[2] using a renormalization-group method has proposed the classification of the growth kinetics of many systems into four classes. In class I, the only influence temperature has on the growth kinetics is through the determination of the correlation length and hence the width of the domain boundaries. In this class the zero-temperature kinetics for sufficiently long-time scales and sufficiently large length scales is the same as the finite-temperature kinetics. In class-II systems domain-growth freezing occurs when the temperature is zero, but the growth kinetics follow a power-law behavior at finite temperatures. Such behavior can result from a time scale τ which depends strongly on the temperature in such a way that $\tau=\tau_0\exp(-E/T)$,where τ_0 is weakly dependent on the temperature T, and E is a local barrier, independent of the domain length. In class-III and class-IV systems, the energy barrier E is dependent on the domain length and there is evidence for logarithmic growth kinetics.

In this investigation we will investigate the zero-temperature growth kinetics for lattice gases with repulsive nearest-neighbor and either attractive or zero second-nearest-neighbor interactions on a triangular lattice and discuss the recently proposed classification[2] as applied to these lattice gases. In previous work it was found that the freezing of domain growth in the eight-state Potts model[4] or the superantiferromagnetic Ising model on a square lattice[5] is caused by the impossibility of kink creation and annihilation for certain values of the interaction parameters. Similar to the eight-state Potts lattice gas on a square lattice, we find two stable "fixed points" at zero temperature. One of them is a freezing "fixed point," and the other is an equilibration "fixed point." These systems exhibit class-II behavior in the scheme proposed recently.[2] We find that freezing of domain growth in the model we study here is caused by fluctuations in the local fractional coverage which can result in the formation of locally stable configurations. These "defects" then pin the domain walls or act as traps for excess local fractional coverage, causing the freezing of domain growth. We also investigated the effect of allowing hops of a range longer than nearest neighbor. We used Kawasaki dynamics (Ref. 14 and additionally in Refs. 15 and 16), and in some simulations allowed not only nearest-neighbor hops but also hops to second and third nearest neighbors. The freezing "fixed point" is rendered unstable by allowing hops of longer range, as in the case of (2×1) domains on a square lattice. Interestingly, we find a growth exponent x of approximately $\frac{1}{3}$ for the equilibration "fixed point." For this model, $x=\frac{1}{3}$ was conjectured by Sadiq and Binder.[9]

II. SIMULATIONS

Since we used Kawasaki dynamics, the probability of a hop is given by

$$P=\begin{cases}0, & \delta E>0\\ \frac{1}{2}, & \delta E=0\\ 1, & \delta E<0\end{cases}, \tag{1}$$

where δE is the change in energy caused by the hop. Time is measured in Monte Carlo steps (MCS) per site. The Hamiltonian of the lattice gases that were simulated is

$$H=J_{\mathrm{NN}}\sum_{(i\neq j)_{\mathrm{NN}}}c_ic_j+J_{\mathrm{NNN}}\sum_{(i\neq j)_{\mathrm{NNN}}}c_ic_j\ . \tag{2}$$

The occupation variable c_i is unity if site i is occupied and zero if it is vacant. The interaction strength of a particle with each of its nearest neighbors is J_{NN}. The second-nearest-neighbor interaction strength is J_{NNN}. We stipulate that J_{NN} is positive, i.e., the nearest-neighbor lateral interaction is repulsive, and the cases $J_{\mathrm{NNN}}=O$ and $J_{\mathrm{NNN}}=-J_{\mathrm{NN}}$ have been studied. The fractional surface coverage used in all the simulations was $\frac{1}{3}$, and at this fractional surface coverage the equilibrium configuration is a single $(\sqrt{3}\times\sqrt{3})$ ordered domain with a degeneracy $p=3$. The phase diagram for $J_{\mathrm{NNN}}=-J_{\mathrm{NN}}$ has been obtained using Monte Carlo simulations.[17] We allowed three different ranges of particle hops, namely: only hops to nearest neighbors, hops to nearest and second-nearest neighbors, and hops to nearest, second-nearest, and third-nearest neighbors. Only hops to vacant sites are allowed. We used lattices which are parallelograms with L sites on each side. The sizes of the lattices used are commensurate with the $(\sqrt{3}\times\sqrt{3})$ structure, and periodic boundary conditions are employed. For each configuration, the individual domain sizes were measured by counting the area occupied by each domain. The average domain size is then calculated, and the square root of this average area is taken to be the characteristic domain length l. For each set of parameters, 30 runs were performed on lattices of size $L\times L=99\times99$ and five runs were performed on lattices size $L\times L=201\times201$. This was done to determine whether the simulations were affected by the finite lattice sizes. For the final domain sizes we obtained, no finite-size effects were observed. Initial configurations were generated by randomly populating the lattices.

III. RESULTS AND DISCUSSION

The results of the simulations employing the Hamiltonian of Eq. (2) with $J_{\mathrm{NNN}}=-J_{\mathrm{NN}}$ are shown in Fig. 1. Each curve is obtained from simulations in which a different range of allowed hops is used. Curve A shows results from simulations where only nearest-neighbor hops are allowed; curve B shows results from simulations in which hops up to second nearest neighbor in range are allowed; and curve C shows results from simulations in which hops up to third nearest neighbor in range are allowed. The asymptotic domain size for the simulations allowing only nearest-neighbor hops is $l\sim16$, and it is independent of the lattice size. The decrease in the growth exponent is perceptibly slower for curves B and C than it is for curve A. Steplike increases in the domain size become apparent toward the end of the runs for the simulations in which hops of up to third nearest neighbor in range are allowed. As we will argue later, domain growth is not frozen if hops of range greater than nearest neighbor are allowed. Simulations were also performed

employing the Hamiltonian of Eq. (2) with a weaker second-nearest-neighbor attractive interaction, $J_{NNN} = -0.1J_{NN}$. In this case only simulations allowing nearest-neighbor hops were performed. The results of these simulations are shown in Fig. 2. The domain growth is frozen as in curve A of Fig. 1. The asymptotic domain size is approximately 18, which is slightly larger ($\sim 10-15\%$) than the asymptotic domain size for $J_{NNN} = -J_{NN}$.

The result of simulations employing the Hamiltonian of Eq. (2) with zero second-nearest-neighbor attraction are shown in Fig. 3, where the curves are labeled according to their allowed hopping ranges as in Fig. 1. The domain-growth kinetics are well described by $l \sim t^x$, with x asymptotically constant in time for all cases. However, as shown in Fig. 3, the value of the growth exponent x increases as the range of allowed hops increases. With only nearest-neighbor hops, the growth exponent is $x \sim 0.33 \pm 0.01$. Increasing the range of allowed hops to include both nearest-neighbor and second-nearest-neighbor hops increases the growth exponent to $x \sim 0.38 \pm 0.01$. Finally, also allowing third-nearest-neighbor hops increases the growth exponent to $x \sim 0.41 \pm 0.01$. Each uncertainty reported here is one standard deviation. The arrows in Fig. 3 indicate the range of data used to fit the growth law for each case.

In Figs. 4(a)–(4d) we show typical configurations that were obtained from the simulations. Each of these configurations was obtained after 1350 MCS per site. The configurations shown in Figs. 4(a)–4(c) were ob-

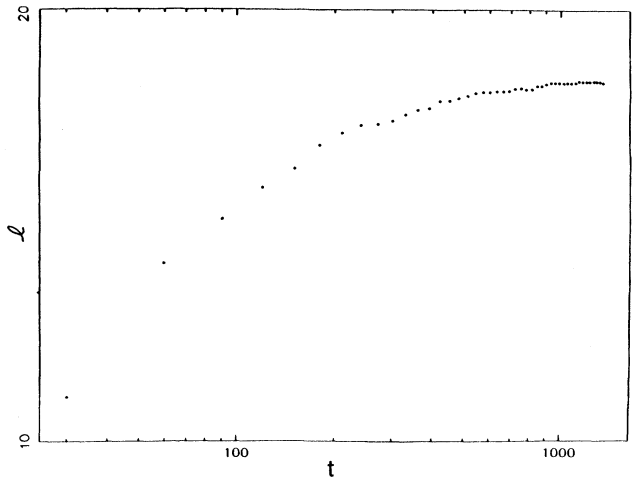

FIG. 2. Results of simulations for domain growth with $J_{NNN} = -0.1J_{NN}$ at $T=0$. Only nearest-neighbor hops are allowed. The ordinate is the average domain length in units of the lattice constant , and the abscissa is the time in units of Monte Carlo steps per site. Notice the freezing of domain growth at an asymptotic domain length slightly larger than that of curve A in Fig. 1.

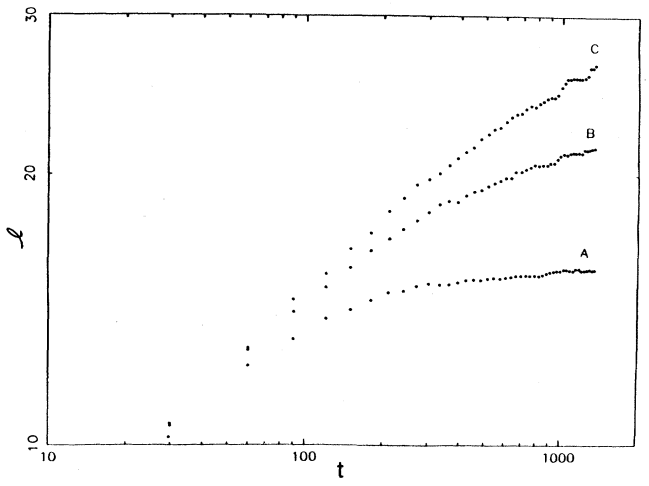

FIG. 1. Results of simulations for domain growth with $J_{NNN} = -J_{NN}$ at $T=0$. The results from simulations with only nearest-neighbor hops allowed are plotted as curve A. The results from simulations with nearest- and second-nearest-neighbor hops allowed are plotted as curve B. The results from simulations with nearest-, second- and third-nearest-neighbor hops allowed are plotted as curve C. The ordinate is the average domain length in units of the lattice constant, and the abscissa is the time in units of Monte Carlo steps per site.

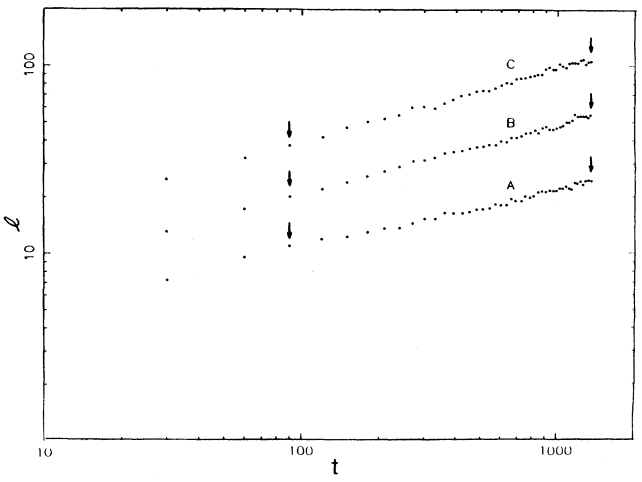

FIG. 3. Results of simulations for domain growth with $J_{NNN} = 0$ at $T=0$. The results from simulations with only nearest-neighbor hops allowed are plotted as curve A. The results from simulations with nearest- and second-nearest-neighbor hops allowed are plotted as curve B. The results from simulations with nearest-, second-, and third-nearest neighbor hops allowed are plotted as curve C. The ordinate and abscissa are the same as those in Fig. 1. For curve B the average domain length l has been multiplied by a factor of 2, and for curve C l has been multiplied by a factor of 4, so that the results can be presented more clearly.

tained from simulations in which there is an attractive second-nearest-neighbor interaction $J_{NNN}=-J_{NN}$. The configuration shown in Fig. 4(a) is obtained from simulations in which only nearest-neighbor hops are allowed, while the configuration shown in Fig. 4(b) is obtained from simulations in which both nearest-neighbor and second-nearest-neighbor hops are allowed, and the configuration shown in Fig. 4(c) is obtained from simulations in which nearest-neighbor, second-nearest-neighbor, and third-nearest-neighbor hops are allowed. These correspond to curves *A*, *B*, and *C* in Fig. 1, respectively. The configuration shown in Fig. 4(d) is obtained from simulations in which the second-nearest-neighbor interaction is zero, and hops of up to third nearest neighbor in range are allowed. The configurations from simulations allowing only nearest-neighbor or second-nearest-neighbor hops are similar.

As the system is quenched to below T_c, $(\sqrt{3}\times\sqrt{3})$ ordered domains form in regions of the lattice where the local fractional coverage is $\frac{1}{3}$. The degeneracy of this structure is $p=3$, and domain walls form between domains which are out of phase with each other. The local configurations at the domain walls are not $(\sqrt{3}\times\sqrt{3})$ superstructures, and the domains will grow to minimize such regions. With second-nearest-neighbor attraction, however, regions which have local fractional coverages greater than $\frac{1}{3}$ will phase separate into domains which are

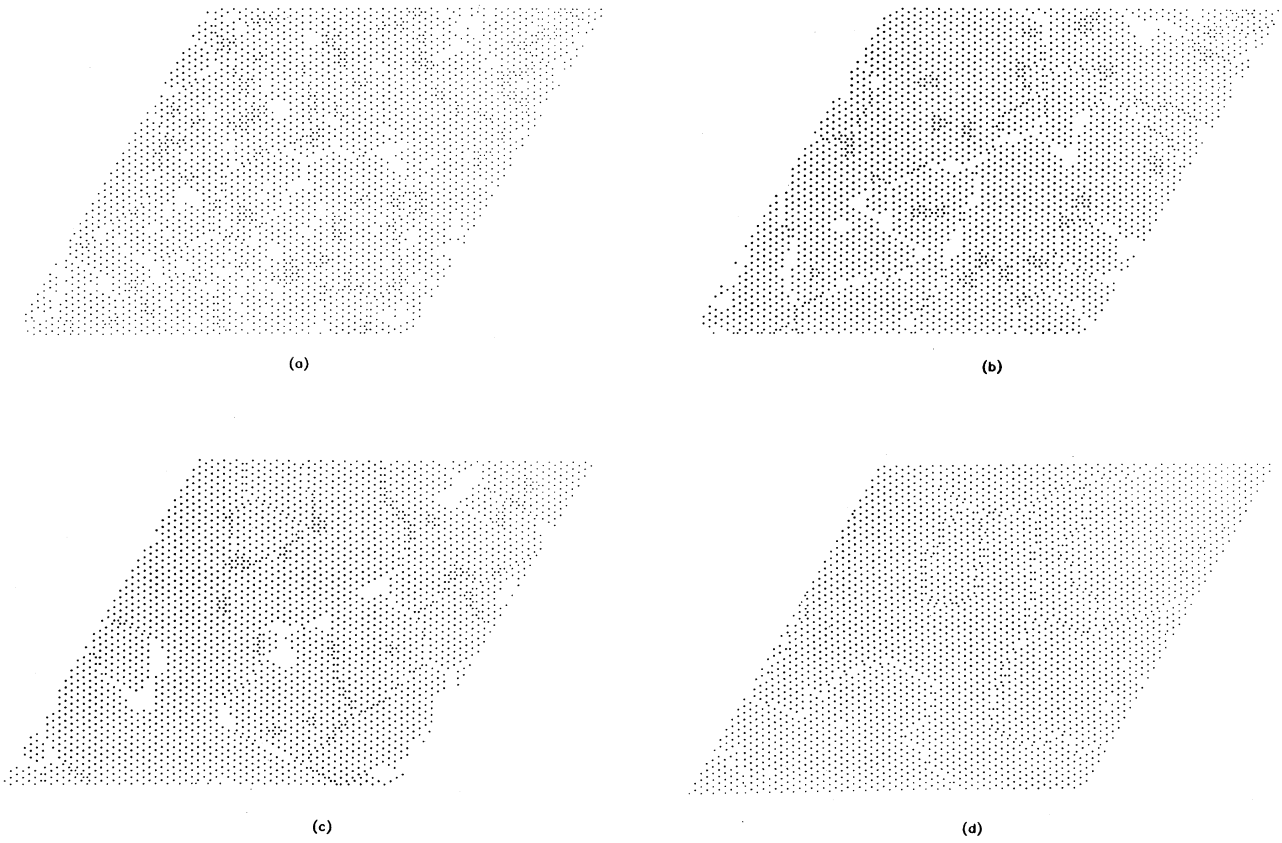

FIG. 4. (a) Typical configuration at a time of 1350 MCS for simulations in which only nearest-neighbor hops are allowed. The second-nearest-neighbor interaction is $J_{NNN}=-J_{NN}$. Note the clusters of ordered $(\sqrt{3}\times\sqrt{3})^*$ particles and clusters of vacant lattices sites. This map corresponds to curve *A* of Fig. 1. (b) Typical configuration at a time of 1350 MCS for simulations in which both nearest- and second-nearest-neighbor hops are allowed. The second-nearest-neighbor interaction is $J_{NNN}=-J_{NN}$. The clusters of ordered $(\sqrt{3}\times\sqrt{3})^*$ particles and clusters of vacant lattice sites are farther apart than in the configuration in (a). The clusters are mobile in this case because second-nearest-neighbor hops are allowed. This map corresponds to curve *B* of Fig. 1. (c) Typical configuration at a time of 1350 MCS for simulations in which first-, second- and third-nearest-neighbor hops are allowed. The second-nearest-neighbor interaction is $J_{NNN}=-J_{NN}$. The clusters of ordered $(\sqrt{3}\times\sqrt{3})^*$ particles and clusters of vacant lattice sites are farther apart than in the configurations in (a) and (b). The mobility of the clusters is larger here than in (b). This map corresponds to curve *C* in Fig. 1. (d) Typical configuration at a time of 1350 MCS for simulations in which hops of up to third-nearest-neighbor sites are allowed. The second-nearest-neighbor interaction is $J_{NNN}=0$. This map corresponds to curve *C* of Fig. 3.

ordered $(\sqrt{3}\times\sqrt{3})$ and clusters which are ordered $(\sqrt{3}\times\sqrt{3})^*$.[10] Similarly, regions in which the local fractional coverages are less than $\frac{1}{3}$ will phase separate into ordered $(\sqrt{3}\times\sqrt{3})$ domains and clusters of vacant lattice sites. This would be expected by considering the phase diagram shown in Fig. 5.[17] The abscissa is the total fractional coverage and the ordinate is the temperature. There is a cusp at the point where the temperature is zero and the total fractional coverage is $\frac{1}{3}$. The equilibrium state at this point is a single ordered $(\sqrt{3}\times\sqrt{3})$ phase, whereas on either side of this point the equilibrium states consist of two phases. When the coverage is less than $\frac{1}{3}$, an ordered $(\sqrt{3}\times\sqrt{3})$ phase is in equilibrium with vacant lattice sites, and when the coverage is greater than $\frac{1}{3}$, an ordered $(\sqrt{3}\times\sqrt{3})$ phase is in equilibrium with an ordered $(\sqrt{3}\times\sqrt{3})^*$ phase. Fluctuations in the local fractional coverage cause excursions into the two-phase regions of the phase diagram. At zero temperature, these fluctuations are shown schematically by arrows in Fig. 5.

Consider the configurations shown in Figs. 4(a)–4(c). These configurations were obtained from simulations in which there is an attractive second-nearest-neighbor interaction between the lattice-gas particles. Clusters of particles showing $(\sqrt{3}\times\sqrt{3})^*$ order as well as "clusters" of vacant lattice sites are clearly observed. These "defects." which are locally stable, are formed via fluctuations in the local fractional coverage as discussed above. It can be seen in Figs. 4(a)–4(c) that some of the "defects" are adsorbed at the interface between different $(\sqrt{3}\times\sqrt{3})$ domains, whereas others are completely embedded in a domain of one phase. For the domain size to grow continuously, it must be possible for a particle to move away from a $(\sqrt{3}\times\sqrt{3})^*$ cluster to regions where there is a deficit in the local fractional coverage. However, to do so a particle must traverse regions which are ordered $(\sqrt{3}\times\sqrt{3})$. The change in energy due to a particle moving away from a $(\sqrt{3}\times\sqrt{3})^*$ cluster into an ordered $(\sqrt{3}\times\sqrt{3})$ domain is positive, however, and the probability of such a move is zero at $T=0$. Similarly, the probability of particles moving from a region which is an ordered $(\sqrt{3}\times\sqrt{3})$ to fill a cluster of vacant sites is zero.

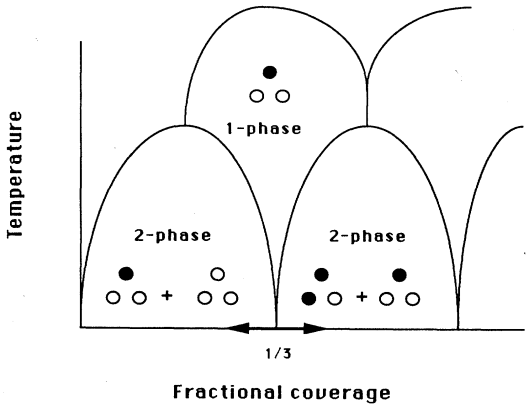

FIG. 5. Schematic of the phase diagram for the lattice gas with $J_{NNN}=-J_{NN}$ on a triangular lattice (Ref. 17). The arrows indicate the fluctuations in the local fractional coverage about a value of $\frac{1}{3}$ at zero temperature, which could produce locally stable clusters of ordered $(\sqrt{3}\times\sqrt{3})^*$ particles or locally stable clusters of vacant sites. The three types of diagrams that are shown indicate local fractional coverages of $\frac{2}{3}$, $\frac{1}{3}$, and zero.

However, if hops of a range longer than nearest neighbor are allowed, it becomes possible for a cluster of ordered $(\sqrt{3}\times\sqrt{3})^*$ particles or a cluster of vacant lattice sites to move as a whole even though no single particle may break away from it. Therefore, in the late stages of the runs, the transport mechanism that enables the domain size to increase is the diffusion of these "defects." As a result of this, the size of a domain will increase in steps of more than one particle each time a cluster of ordered $(\sqrt{3}\times\sqrt{3})^*$ particles "collides" with a cluster of vacant lattice sizes. The effect of such discontinuities can be clearly observed, toward the end of the runs, in curve C of Fig. 1. Hence, even allowing only finite-range hops, domain growth is not frozen so long as hops of a range longer than nearest neighbor are allowed. The diffusivity of the "defects" is larger in the case in which third-nearest-neighbor hops are allowed than in the case in which second-nearest-neighbor hops are allowed. Thus, the configuration shown in Fig. 4(c) is more "aged" than that shown in Fig. 4(b) even though both were obtained after the same number of Monte Carlo moves in the simulations. Consequently, the latter configuration shows a larger number of smaller "defect" clusters which are separated by shorter distances. It is possible that both curve B and curve C of Fig. 1 shows $l\sim t^x$ behavior for long times. However, our simulations are not sufficiently long to verify this. There is, however, no reason to expect that $x\sim\frac{1}{3}$ since the mechanism of growth is not diffusion of single particles but rather of "defects," the sizes of which must increase with time, and the diffusivity of which must decrease with size. With an infinite range of allowed hops, particles can go from the $(\sqrt{3}\times\sqrt{3})^*$ clusters directly to the clusters of vacant lattice sites. Since the change in energy for such a move is not positive, the probability is not zero. Hence, with a range of allowed hops extended to infinite distance, domain freezing does not occur.

Since it is the second-nearest-neighbor attractive interaction which is responsible for the formation of the "defects," it is interesting to consider the case in which this interaction is set to a weaker attraction or to zero. From the above considerations, we expect that, for simulations in which only nearest-neighbor hops are allowed, domain growth will be frozen as long as the second-nearest-neighbor interaction is attractive. This is because the clusters of vacant lattice sites and the clusters of particles in the ordered $(\sqrt{3}\times\sqrt{3})^*$ domains are locally stable as long as J_{NNN} is negative. Furthermore, with only nearest-neighbor hops allowed, these clusters are not mobile. The results shown in Fig. 2 support this conclusion. The domain size is frozen at $l\sim 18$.

With zero second-nearest-neighbor attraction, clusters of $(\sqrt{3}\times\sqrt{3})^*$ and clusters of vacant lattice sites are not locally stable. Consider the configuration shown in Fig. 4(d), which is obtained from simulations in which the

lattice-gas particles have zero second-nearest-neighbor interaction. In contrast to Figs. 4(a)–4(c), we do not observe clusters of ordered $(\sqrt{3}\times\sqrt{3})^*$ particles or clusters of vacant lattice sites. Thus there are no "defects," as in the case of $J_{\rm NNN}<0$, to pin the domain walls or to trap excess or deficit local fractional coverage. Hence, domain freezing is released by decreasing the second-nearest-neighbor interaction to zero. It can be seen that the boundaries between domains consist of *walls* with either excess or deficit fractional local coverage, and it is interesting to note that the growth exponent is $x\sim\frac{1}{3}$ for the case in which only nearest-neighbor hops are allowed (cf. curve A of Fig. 3). This value for the growth exponent was conjectured by by Sadiq and Binder[9] on the basis of their simulations which indicated that when there are domain walls with excess or deficit local fractional coverage, the redistribution of the excess and deficit density over a length scale of l results in $x\sim\frac{1}{3}$. Our results support this conjecture. It has been suggested that the true density-conserved growth exponent for (2×1) domains on a square lattice is $x\sim\frac{1}{2}$, and the values obtained by Sadiq and Binder[9] resulted from a "crossover" between $x=0$ and $x\sim\frac{1}{2}$.[6] For the lattice gas that we studied, there is no freezing of domain growth at zero temperature without second-nearest-neighbor attraction. Thus the simulation result of $x\sim\frac{1}{3}$ can be a true growth exponent and does not have to arise from a crossover effect between $x=0$ and $\frac{1}{2}$.

For simulations in which $J_{\rm NNN}=0$, increasing the range of allowed hops from nearest neighbor to third nearest neighbor increases the measured growth exponent from ~0.33 to ~0.41, (cf. Fig. 3). This is similar to the increase in the growth exponent from $x=0$ to $x\sim0.5$ that was observed for the ordering of (2×1) domains on a square lattice when the range of allowed hops is increased from nearest neighbor to second nearest neighbor.[6] The latter result led to the conclusion that the growth exponent for density-conserved growth is $\frac{1}{2}$, regardless of the degeneracy of the ground state. It was also suggested that earlier work[9] obtained $x\sim\frac{1}{3}$ because of the influence of "crossover" from $x=0$ at zero temperature when only nearest-neighbor hops are allowed, and that the simulations had not reached the asymptotic regime where $x=\frac{1}{2}$, this regime being reached faster when hops of longer range are allowed.[6] However, even for the case in which only nearest-neighbor hops are allowed, we have found that domain growth for the Hamiltonian with $J_{\rm NNN}=0$ is not frozen at zero temperature. Thus, there is no possibility of a "crossover" from $x=0$ to $\frac{1}{2}$ as the range of hops is increased. Hence, if the density-conserved growth exponent is $x=\frac{1}{2}$, even for $p>2$, then this is the value that would be observed even for the case in which only nearest-neighbor hops are allowed. However, we actually observed $x\sim0.33$.

Our results for the growth of $(\sqrt{3}\times\sqrt{3})$ domains on a triangular lattice and those obtained earlier[6,9] for the growth of (2×1) domains on a square lattice may be better interpreted as follows. If there is a need for redistribution of either excess or deficit local density then, as suggested by Sadiq and Binder,[9] the growth exponent is $x\sim\frac{1}{3}$, allowing only nearest-neighbor hops. If the Hamiltonian is such that freezing occurs at zero temperature, then the growth exponent at temperatures close to zero is affected by "crossover" from $x=0$.[9] Increasing the range of allowed hops changes the mechanism of transport from diffusion to evaporation-condensation. This is because the limit in which hops of all possible lengths up to infinity are allowed in Kawasaki dynamics is equivalent to Glauber dynamics.[13]

For the simulations that we performed, the largest lattice size was 201×201, and there is certainly some doubt as to whether the values of x obtained are the asymptotic growth exponents. It is, however, suggestive that the growth exponent obtained from simulations allowing only nearest-neighbor hops is in excellent agreement with the Lifshitz-Slyozov result of $x=\frac{1}{3}$ for diffusion driven coarsening during the late stages of phase separation in solid solutions.[18,19] Furthermore, it is not clear how a change in the length scale of the hops from nearest neighbor to second nearest neighbor can produce a "crossover" from $x\sim\frac{1}{3}$ to $x=\frac{1}{2}$. Therefore, we conclude that the growth exponent for density-conserved growth is not $\frac{1}{2}$, but changes continuously from $x\sim\frac{1}{3}$ to $x=\frac{1}{2}$ as the length of allowed hops increases from nearest neighbor to infinity.

It is clear that the case in which $J_{\rm NNN}=0$ falls into class-I (Ref. 2) systems, whereas the case in which $J_{\rm NNN}=-J_{\rm NN}$ exhibits class-II behavior. Without next-nearest-neighbor attraction the time scale of the lattice gas is not strongly dependent on the temperature through an energy barrier. On the other hand, with next-nearest-neighbor attraction, the time scale is dependent on the temperature through an energy barrier which is not a function of the domain size. Consider the configuration space of the system. The local stability of clusters of vacant sites and clusters of ordered $(\sqrt{3}\times\sqrt{3})^*$ particles imply that there are points in configuration space which have energies lower than all other points that it can access if only nearest-neighbor hops are allowed. Thus, in order for the system to "escape" from such traps an energy barrier, independent of the domain size, has to be overcome. Therefore, the time scale for such a lattice gas would be strongly dependent on the temperature, and freezing occurs when the temperature is zero. Therefore, the triangular lattice gas with $J_{\rm NN}=-J_{\rm NNN}$ is a class-II system[2] when only nearest-neighbor hops are allowed. When hops of longer range are allowed, from any point in configuration space there are always accessible points with lower or equal energies. Hence, freezing does not occur, and the lattice gas is a class-I system. Therefore, the range of hops that is allowed for a lattice-gas particle can subtly influence the dynamical connectivity of points in configuration space, and is an important parameter to consider in classifying growth kinetics.

IV. CONCLUSIONS

We have found that for a triangular lattice gas with a fractional surface coverage of one-third and with nearest-neighbor repulsions, the nature of domain growth

of $(\sqrt{3}\times\sqrt{3})$ superstructures is sensitively dependent upon whether the second-nearest-neighbor interaction is zero or attractive. When the second-nearest-neighbor interaction is attractive, fluctuations in the local fractional coverage lead, upon quenching to zero temperature, to the formation of locally stable clusters with a $(\sqrt{3}\times\sqrt{3})^*$ superstructure (two particles per unit cell) and clusters of vacant lattice sites. In simulations allowing only nearest-neighbor hops, single lattice-gas particles cannot break away from the ordered $(\sqrt{3}\times\sqrt{3})^*$ clusters, and single vacant sites cannot break away from the clusters of vacant lattice sites because both these clusters are locally stable. As a result, domain growth freezes. However, when hops of a range longer than nearest neighbor are allowed, the freezing is released. In this case it is also true that single particles cannot break away from the ordered $(\sqrt{3}\times\sqrt{3})^*$ clusters and single vacant sites cannot break away from the clusters of vacant sites. However, both the ordered $(\sqrt{3}\times\sqrt{3})^*$ clusters and the clusters of vacant lattice sites are mobile. This is because single particles at the boundary of an ordered $(\sqrt{3}\times\sqrt{3})^*$ cluster can move along the boundary, by hopping from their original sites to second-nearest-neighbor sites, and still remain part of the cluster. Such hops, which do not result in a change in the total energy and hence have a probability of $\frac{1}{2}$, are forbidden when only nearest-neighbor hops are allowed. Similarly, single vacant sites can hop along the boundary of the clusters of vacant lattice sites. Toward the end of the simulation runs that we performed, the "coalescence" of these "defect" clusters to form ordered $(\sqrt{3}\times\sqrt{3})$ superstructures contributes significantly to domain growth. In the classification of growth kinetics, it is thus important to consider the range of hops that are allowed for lattice-gas particles (or the range of spin exchange for Ising system). In the systems we have studied here, a change of hop range from nearest neighbor to merely next nearest neighbor can change the domain growth behavior from class I to class II in the scheme proposed in Ref. 2.

Without an attractive second-nearest-neighbor interaction, domain growth is not frozen even at zero temperature. We find a growth exponent of $x\sim\frac{1}{3}$ when only nearest-neighbor hops are allowed, in agreement with the conjecture by Sadiq and Binder.[9] It has been argued that the value of $x\sim\frac{1}{3}$ for the growth of (2×1) domains on a square lattice results from a crossover effect between $x=0$ at zero temperature and $x=\frac{1}{2}$ at finite temperature.[6] Our results indicate that even without the freezing of domain growth at zero temperature, it is possible to have a growth exponent of $x\sim\frac{1}{3}$. In agreement with results for the growth of (2×1) domains on a square lattice,[6] we find that the observed growth exponent depends on the range of allowed hops. However, we interpret this as a continuous dependence of the growth exponent on the hopping range rather than a crossover effect. This is more consistent because we do not observe domain freezing even in the case in which we allow only nearest-neighbor hops. We also note that in the case in which density is conserved (Kawasaki dynamics), allowing the range of hops to be infinitely long causes the system effectively to evolve according to Glauber dynamics, since simulations are always done on finite lattices. Therefore, $x=\frac{1}{2}$ when the range of allowed hops is infinitely long, even though density is conserved. We conclude that by increasing the range of allowed hops from nearest neighbor to infinity, the growth exponent changes from $x\sim\frac{1}{3}$ to $x=\frac{1}{2}$.

ACKNOWLEDGMENTS

This research was supported by the National Science Foundation under Grant No. CHE-8617826. We acknowledge partial support by the Donors of the Petroleum Research Fund (PRF 19819-AC5-C).

*Present address: Department of Chemical Engineering, University of California, Santa Barbara, Santa Barbara, CA 93106.

[1]K. Binder and D. W. Heermann, in *Scaling Phenomena in Disordered Systems,* edited by R. Pym and A. Skjeltorp (Plenum, New York, 1985); K. Binder, D. W. Heermann, A. Milchev, and A. Sadiq, in *Heidelberg Colloquium on Glassy Dynamics and Optimization,* edited by J. L. van Hemmen and I. Morgenstern (Springer, Berlin, 1987).

[2]Z. W. Lai, G. F. Mazenko, and O. T. Valls, Phys. Rev. B **37**, 9481 (1988).

[3]G. F. Mazenko, O. T. Valls, and F. C. Zhang, Phys. Rev. B **31**, 4453 (1985).

[4]J. Vinals and J. D. Gunton, Phys. Rev. B **33**, 7795 (1986).

[5]A. Host-Madsen, P. J. Shah, T. V. Hansen, and O. G. Mouritsen, Phys. Rev. B **36**, 2333 (1987).

[6]H. C. Fogedby and O. G. Mouritsen, Phys. Rev. B **37**, 5962 (1988).

[7]Here, J_{NN} is the nearest-neighbor interaction energy, and $s_i=\pm1$ is the spin of the ith lattice site.

[8]Here, J_{NNN} is the next-nearest-neighbor interaction energy, and δ is the Kronecker δ.

[9]A. Sadiq and K. Binder, J. Stat. Phys. **35**, 517 (1984).

[10]We use $(\sqrt{3}\times\sqrt{3})$ as an abbreviation for the $(\sqrt{3}\times\sqrt{3})R30°$ superstructure. The structure with two particles and one vacancy rather than two vacancies and one particle per unit cell is denoted by $(\sqrt{3}\times\sqrt{3})^*$.

[11]H. C. Kang and W. H. Weinberg (unpublished).

[12]H. Binder, Ber. Bunseges. Phys. Chem. **90**, 257 (1986).

[13]H. C. Kang and W. H. Wienberg, Phys. Rev. B **38**, 11 543 (1988).

[14]Kawasaki dynamics, rather than a proper energy-barrier model (Refs. 15 and 16), were employed since the case of zero temperature is being investigated.

[15]E. S. Hood, B. H. Toby, and W. H. Weinberg, Phys. Rev. Lett. **55**, 2437 (1985).

[16]H. C. Kang and W. H. Weinberg, J. Chem. Phys. **90**, 2824 (1989).

[17]D. P. Landau, Phys. Rev. B **27**, 5604 (1983).

[18]I. M. Lifshitz and V. Slyozov, J. Phys. Chem. Solids **19**, 35 (1961).

[19]I. M. Lifshitz, Zh. Eksp. Teor. Fiz. **42**, 1354 (1962) [Sov. Phys.—JETP **15**, 939 (1962)].